Songklanakarin J. Sci. Technol.
43 (2), 582-587, Mar. - Apr. 2021

http://www.sjst.psu.ac.th

Original Article

Green synthesis of cerium oxide nanoparticles using *aloevera leaf* extract and its optical properties

S. Sebastiammal[1], S. Sonia[1], J. Henry[2], and A. Lesly Fathima[1*]

[1] *Department of Physics, Holy Cross College (Autonomous), Nagercoil, Tamil Nadu, 629004 India*

[2] *Department of Physics, Manonmaniam Sundaranar University, Abishekapatti, Tirunelveli, Tamil Nadu, 627012 India*

Received: 11 February 2020; Revised: 20 March 2020; Accepted: 13 April 2020

Abstract

In the present report, bio-reduction of cerium nitrate into cerium oxide nanoparticles has been done using *aloevera* leaf extract. The synthesized CeO_2 nanoparticles were characterized by PXRD, FTIR, UV-DRS, FESEM, EDAX and PL. From the PXRD analysis, it is found that the synthesized CeO_2 nanoparticles were the face centered cubic structure. The crystalline size is found to be about 7 nm and 12 nm for the CeO_2 nanoparticles before and after calcination respectively. FTIR spectra exhibit the formation of CeO_2 nanoparticles. The UV – Vis spectra shows an absorption peak at 320 nm. The FESEM analysis, showed spherical shaped CeO_2 nanoparticles and its size is about 50 nm.

Keywords: biosynthesis, CeO_2 NPs, PXRD, FTIR, UV-DRS, FESEM

1. Introduction

There is an increasing commercial demand for nanoparticles due to its promising applications in electronics, chemistry, catalysis, energy and medicine (Bar *et al.*, 2009; Mittal & Pandey, 2014). Metallic nanoparticles are traditionally synthesized by wet-chemical techniques, where the chemicals used are quit toxic and inflammable (Edison & Sethuraman, 2013). Cerium is one of the most abundant rare-earth metals found in the Earth's crust (Nisha *et al.*, 2014). Cerium oxide (CeO_2) has received much attention in the global nanotechnology market due to its useful applications for catalysts, fuel cells, and fuel additives (Bankar, Joshi, Kumar, & Zinjarde, 2010). CeO_2 is a semiconductor with wide band gap energy (3.19 eV) and large exciton binding energy (Arumugam *et al.*, 2015). Recently the CeO_2 NPs were used as a diesel fuel additive, to reduce the ignition temperature of carbonaceous diesel exhaust particle (DEP) and subsequently to reduce the emission of particulate matter from diesel engines (Niu, Azfer, Rogers, Wang, & Kolattukudy, 2007). Cerium oxide nanoparticles are exhibiting excellent antioxidant properties so that they can be able to cure stress-related diseases (Caputo *et al.*, 2017).

Green nanotechnology is a mushrooming area of research in the scientific world. The green synthesis method offers a plenty of advantages such as cost-effectiveness, large scale commercial production and pharmaceutical applications. The plant extract which facilitates green synthesis has gained a wide attention and has emerged as an active research area in the field of nanotechnology. Plant extract consists of tannins and poly phenol which are widely applied in food processing as natural additives to edible foods and in leather industry for fabrication. The polyphenolic OH^- groups have good affinity towards metal ions; hence the plant extract is widely applied as reducing, stabilizing and chelating agent (Kalaiselvi, Mathammal, Vijayakumar, & Vaseeharan, 2018). Arunachalam, Karpagasundaram, and Rajarathinam, (2017) have prepared *Prosopis juliflora* leaf extract mediated CeO_2 nanoparticles and studied its antibacterial activity

*Corresponding author
Email address: leslysat@gmail.com,
leslyfathima@holycrossngl.edu.in

(Arunachalam, Karpagasundaram, & Rajarathinam, 2017). Arumugam *et al.* (2015) prepared CeO_2 NPs using *Gloriosa superba L*. leaf extract (Arumugm *et al.*, 2015). Thovhogi, Diallo, Gurib-Fakim, and Maaza, (2015) prepared CeO_2 NPs using *Hibiscus Sabdariffa* flower extract (Thovhogi, Diallo, Gurib-Fakim, & Maaza, 2015). Kannan and Sundrarajan, (2014) studied the antibacterial effect of CeO_2 NPs synthesized using *Acalypha indica* leaf extract (Kannan & Sundrarajan 2014).

In the present report we have used *aloevera* leaf extract for the synthesis of CeO_2 NPs and it is potentially advantageous over microorganisms or plant extracts due to its simplicity, less bio-hazard and complicated process of maintaining cell culture (Kaviyarasu *et al.*, 2017; Mariappan, Pandi, Balasubramanian, Palanichamy, & Neyvasagam 2017). Many researchers have used the *Aloevera* extract for the synthesis of nanoparticles and studied its antibacterial, antifungal, and mosquitocidal activity (Karimi, J., & Mohsenzadeh, 2015; Kumar, Shameem, Kollu, Kalyani, & Pammi, 2015; Muralikrishna, Pattanayak, & Nayak, 2014; Vélez *et al.*, 2018). *Aloevera* extract has substances that lead to steric repulsion between individuals preventing nanoparticles from aggregation using *Aloeve*ra as surfactant prevents nuclei aggregation by decreasing the total surface energy because it contains a multitude of chemical constituents such as amino acids, enzymes, minerals, vitamins anthraquinones, lignin, monosaccharide, polysaccharides, salicylic acid, saponins, sterols, and minerals (Vélez et al., 2018). This motivated the authors to synthesis of CeO_2 NPs is the new facelift towards green nanotechnology, because of its eco-friendly, economical and rapid approach. Moreover, the use of *Aloevera* leaf extract can tune the optical properties of CeO_2 NPs. Hence the present work focuses on preparing such eco-friendly material CeO_2 by green synthesis route and to study the optical properties of the synthesized nanoparticles.

2. Experimental

Leaves from *Aloe barbadensis* miller plant were collected and washed thoroughly with water to remove any dirt or debris on the surface. Rind from the leaves was carefully peeled off using a sharp knife and discarded. The leaf was slitted longitudinally into half and sharp edged spoon was used to scrap off the gel. The gel was put into a sterile beaker. It was stirred well to get the *aloevera* extract. Then, 0.5 M of Cerium (III) nitrate hexahydrate was taken in a beaker and 50 ml of distilled water was added to it. This solution was stirred using a magnetic stirrer until a homogeneous solution was formed. With this aqueous solution, 50 ml of *aloevera* leaf extract was added. The reaction mixture was stirred for 30 minutes continuously. The solution was heated on a hot plate at 80 °C till the supernatant got evaporated. The obtained product was pounded into fine powder and calcined at 600 °C for 2 hours.

The crystal structures of the obtained products were characterized by studying the X-ray diffraction pattern (PANalytical X'pert Pro with CuK_α (λ=1.5406 Å). The morphology and elemental composition of the samples were analyzed using a field emission scanning electron microscope (FEI QUANTA-250). Absorption spectra (JASCO V-650 Spectrophotometer) were used to analyze the optical properties of the prepared nanostructures. Fourier transform infra-red spectrum (Bruker IFS 48) was recorded in the range of 4,000-400 cm^{-1} and was used to identify the functional groups present in CeO_2 nanoparticles.

3. Results and Discussion

Figure 1(a) depicts the PXRD pattern of the as-prepared CeO_2 NPs that shows polycrystalline peaks at 2θ = 28.66°, 32.43°, 47.25°, 56.20°, 69.52°, and 76.06° corresponding to the diffraction of (111), (200), (220), (311), (400), and (331) planes which belongs to the cubic structure of CeO_2 NPs (JCPDS file No: 81-0792). Figure 1(b) depicts the PXRD pattern of CeO_2 NPs calcinated at 600 ºC. It also exhibits the same PXRD profile, however the intensity of the crystalline peaks gets increased. The results well agreed with the earlier reports of CeO_2 ananoparticles (Anand, Muthuvel, Mohana, Anandhi, & Pavithra, 2018; Aseyd, Es-haghi, & Tabrizi, 2019). The crystallite size of CeO_2 NPs was estimated from the Scherer's equation (Aljuboori, 2018)

$$D = \frac{0.9\,\lambda}{\beta\,cos\theta} \quad (1)$$

and it is found to be about 7 nm and 12 nm for as synthesized and calcinated samples, respectively. The calcinated CeO_2 NPs shows higher crystrallite size due to more energy which is given to the atoms to diffuse and reside at the suitable site in the crystal lattice, and grains with less surface energy that will become larger at elevated temperature (Kayani, Saleemi, & Batool 2015).

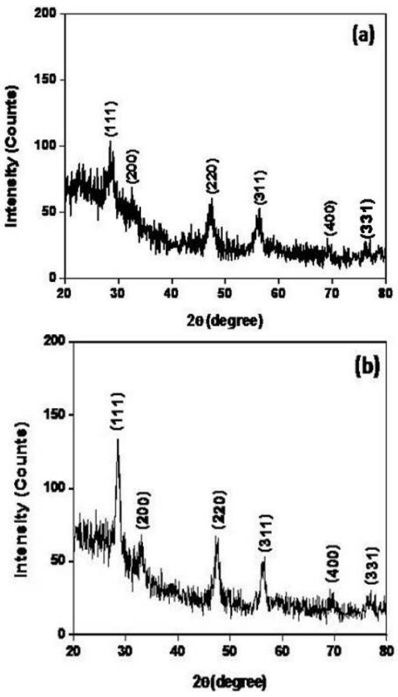

Figure 1. PXRD pattern of a) as synthesized and b) calcinated CeO_2 NPs.

Figure 2(a) & (b) shows the FTIR spectra of as synthesized and calcinated CeO_2 NPs. The FTIR spectra show a band in the range 3,700 cm^{-1} to 3,000 cm^{-1} that is due to O-H

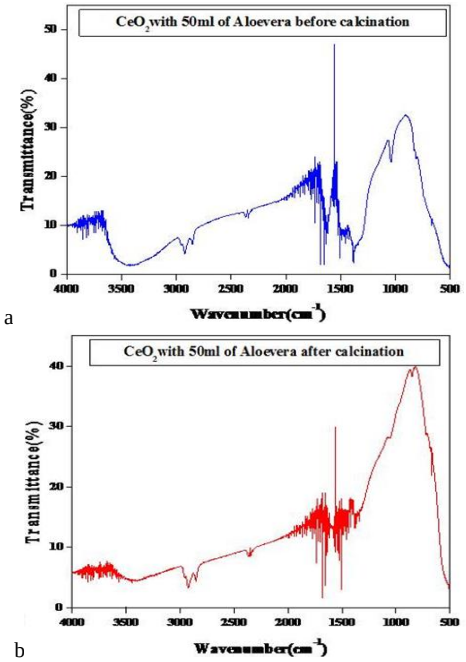

Figure 2. FTIR spectra for a) as synthesized and b) calcinated CeO_2 NPs.

stretching (Arunachalam *et al.*, 2017). The intensity of the peak gets reduced after calcination. The peak observed at 2,420 cm^{-1} and 1,380 cm^{-1} is due to the presence of C=O (Arumugam *et al.*, 2015). The peak at 858 cm^{-1} and 530 cm^{-1} is due to Ce-O stretching vibration (Babitha, Sreedevi, Priyanka, Sabu, & Varghese, 2015). The band at 1,647 cm^{-1} corresponds to the bending of H–O–H which is partly overlapping the O–C–O stretching band (Arumugam *et al.*, 2015).

Figure 3(a) & (b) shows the UV-Vis spectra of as synthesized and calcinated CeO_2 NPs. The higher absorption at 200 nm to 400 nm indicates that the absorption of CeO_2 nanoparticles is in UV region. The optical band gap energy (E_g) of the CeO_2 nanoparticles was estimated using the equation (Aljuboori, 2018):

$$\alpha h\nu = A\,(h\nu - E_g)^n \qquad (2)$$

where, α is the absorption coefficient, hν is the discrete photon energy, A is a constant, and E_g is the band gap of the material. The value of n is ½ and 2 for direct allowed and indirect allowed transitions, respectively. The band gaps of the samples can be obtained by plotting $(\alpha h\nu)^2$ versus hν in the high absorption range followed by extrapolation of the linear portion of the absorption edge to find the intercept on the X-axis as shown in Figure 4 (a-b) . The band gap value is found to be 3.33 eV and 3.32 eV for as synthesis and calcinated CeO_2 NPs. It is observed that the band gap value decreases during the calcination process which may be due to the increase in particle size. The obtained band gap value is well agrees with the earlier report of CeO_2 NPs. The obtained band gap value is found to be lower than the CeO_2 nanoparticles prepared using *Momordica Charantia* leaf extract (Anand *et al.*, 2018), *Gloriosa superb* leaf extract (Arumugam *et al.*, 2015).

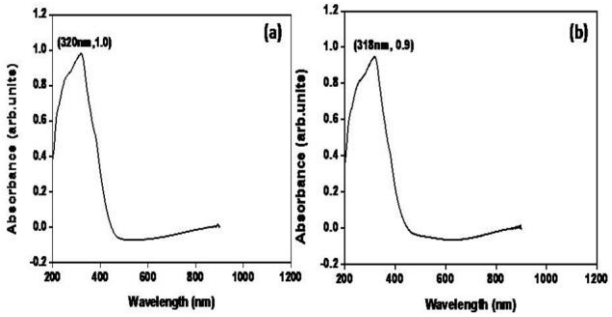

Figure.3 UV-Vis spectra of a) as synthesized and b) calcinated CeO_2 NPs.

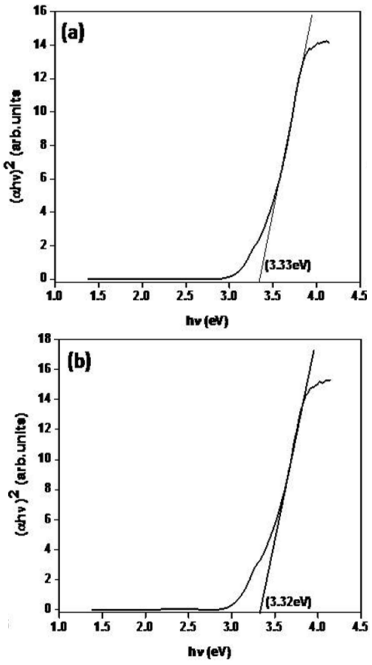

Figure 4. Tauc plot of a) as synthesized and b) calcinated CeO_2 NPs.

Figure 5 represents FESEM images of calcinated CeO_2 NPs with different magnifications (20,000X, 40,000X, and 80,000X). It is observed that the small sized (~50 nm) nanoparticles were formed after the annealing process. The chemical compositions of as-prepared CeO_2 NPs were investigated by EDAX analysis (Figure 6). It shows that the 42.05% of Cerium (Ce) and 57.95% of Oxygen (O) were present in the prepared nanoparticles. These results confirmed the formation of green synthesized NPs with no impurity in their composition. Similar result is observed for the CeO_2 nanoparticles prepared using *Moringa olifera* extract (Mahmud, 2016).

The calculated crystallite size from the XRD is smaller than that of FESEM. The observed difference is attributed to the fact that XRD measurements consider crystallite sizes as sizes of "coherently diffracting domains" of crystals while grains may contain several of these domains. Another reason for these differences could be a possible Plasmon interaction of SEM electron bundle with Ag-nano particle surface, which appears in magnification size effect (Dimitrijević *et al.* 2013).

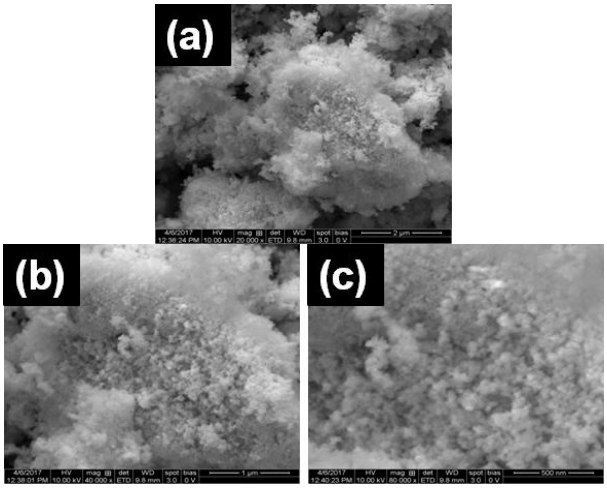

Figure 5. FESEM image of CeO_2 NPs calcinated at 600 °C with a magnification (20,000X, 40,000X, 80,000X).

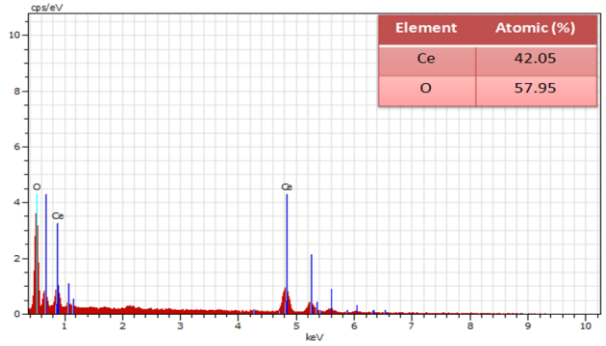

Figure 6. EDAX spectrum for CeO_2 NPs calcinated at 600 °C.

Figure 7 depicts the photoluminescence (PL) emission spectra for calculated samples recorded with the excitation peak of wavelength 409 nm. The PL spectrum show ten emission peaks at 361 nm, 376 nm, 388 nm, 409 nm, 438 nm, 461nm, 492 nm, 519 nm, 542 nm, and 589 nm. The peaks 361 nm, 376 nm, and 388 nm correspond to near band edge emission which is attributed to a band-to-band recombination process, possibly involving localized or free excitons (Wang, Ren, Liu, Lu, & Wang 2011). The peak 409 nm corresponds to violet that originates from the defect states existing extensively between the Ce 4f state and O 2p valence band (Morshed *et al.*, 1997). These defects possibly act as radiative recombination centers for electron initially excited from the valence band to the 4f band of the CeO_2 (Chen, Zu, Xiang, & Zhang, 2007). The blue emissions peak observed at 438 nm and 461 nm is related to the abundant defects such as dislocations, which is helpful for fast oxygen transportation. Ce 4f level with a width of 1 eV is localized at the forbidden gap, which lies at 3 eV over the valence band (O 2p). At room temperature, electron transition mainly occurs from defects level to O 2p level (Chai, Yang, Liu, Liao, & Chen, 2003). The blue–green emission is located at 492 nm is possibly due to surface defects in the CeO_2 NPs, and the low intensity of the green emission may be due to the low density of oxygen vacancies (Arumugam *et al.*, 2015). The emission peak at 519 nm is due to the radiative recombination of excitions and the

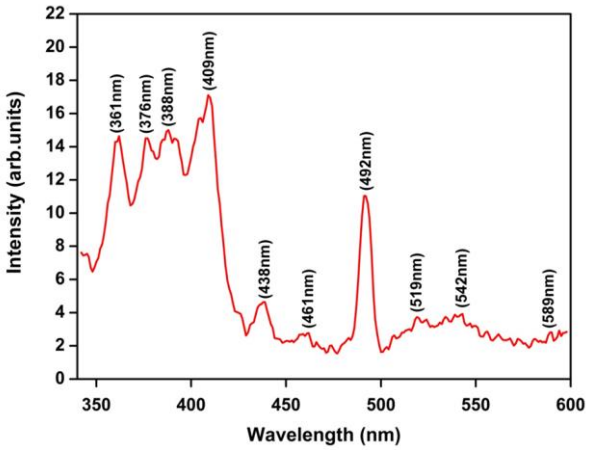

Figure 7. PL emission spectrum of calcinated CeO_2 NPs

surface defects are existing between Ce the inner 4f-5d transition and O 2p valence state (Mobeen, & Sundaram, 2019). The emission peak at 542 nm and 589 nm might be because of surface defects in the CeO_2 NPs, and the less intense emerald emission can be related with oxygen vacancies (Sisubalan *et al.*, 2018).

4. Conclusions

The green synthesis has been adopted to prepare CeO_2 NPs using *aloevera* leaf extract which are better alternative to chemical synthesis, without using any hazardous chemical, reducing agent and capping agent. The PXRD result confirms the formation of face centered cubic phase of CeO_2 NPs. The CeO_2 NPs annealed at 600 °C shows higher crystallinity and crystallite size. UV-DRS analysis shows that the presence of blue shift is due to quantum confinement effect. FESEM images showed that the synthesized CeO_2 NPs are of nanocrystal shaped morphology. EDAX spectrum confirms the purity of the samples.

References

Aljuboori, M. S. H. (2018). Study of optical and structural properties of NiO thin films prepared by chemical spray pyrolysis (CSP) Method. *Jordan Journal of Physics*, *11(3)*, 147-152.

Anand, B., Muthuvel, A., Mohana, V., Anandhi, S., & Pavithra, M. (2018) Effect of chemically synthesis compared to biosynthesized CeO_2 NPS using aqueous extract of *Momordica Charantia*, *International Journal for Research in Applied Science and Engineering Technology*, *6*, 1073-1079.

Arumugam, A., Karthikeyan, C., Hameed, A. S. H., Gopinath, K., Gowri, S., & Karthika, V. (2015). Synthesis of cerium oxide nanoparticles using *Gloriosa superba L.* leaf extract and their structural, optical and antibacterial properties. *Materials Science and Engineering: C*, *49*, 408-415.

Arunachalam, T., Karpagasundaram, M., & Rajarathinam, N. (2017). Ultrasound assisted green synthesis of cerium oxide nanoparticles using *Prosopis juliflora* leaf extract and their structural, optical and

antibacterial properties. *Materials Science-Poland, 35*(4), 791-798.

Aseyd Nezhad, S., Es-haghi, A., & Tabrizi, M. H. (2019) Green synthesis of cerium oxide nanoparticle using *Origanum majorana* L. leaf extract, its characterization and biological activities. *Applied Organometallic Chemistry, 34*, e5314. doi:10. 1002/aoc.5454.

Babitha, K. K., Sreedevi, A., Priyanka, K. P., Sabu, B., & Varghese, T. (2015). Structural characterization and optical studies of CeO_2 nanoparticles synthesized by chemical precipitation. *Indian Journal of Pure and Applied Physics, 53*(9), 596-603.

Bankar, A., Joshi, B., Kumar, A. R., & Zinjarde, S. (2010). Banana peel extract mediated novel route for the synthesis of silver nanoparticles. *Colloids and Surfaces A: Physicochemical and Engineering Aspects, 368*(1-3), 58-63. doi:10.1016/j.colsurfa. 2009.07.021.

Bar, H., Bhui, D. K., Sahoo, G. P., Sarkar, P., Pyne, S., & Misra, A. (2009). Green synthesis of silver nanoparticles using seed extract of *Jatropha curcas*. *Colloids and Surfaces A: Physicochemical and Engineering Aspects, 348*(1-3), 212-216.

Caputo, F., Mameli, M., Sienkiewicz, A., Licoccia, S., Stellacci, F., Ghibelli, L., & Traversa, E. (2017). A novel synthetic approach of cerium oxide nanoparticles with improved biomedical activity. *Scientific Reports, 7*(1), 1-13.

Chai, C., Yang, S., Liu, Z., Liao, M., & Chen, N. (2003). Violet/blue photoluminescence from CeO_2 thin film. *Chinese Science Bulletin, 48*(12), 1198-1200.

Chen, M. Y., Zu, X. T., Xiang, X., & Zhang, H. L. (2007). Effects of ion irradiation and annealing on optical and structural properties of CeO2 films on sapphire. *Physica B: Condensed Matter, 389*(2), 263-268.

Dimitrijević, R., Cvetković, O., Miodragović, Z., Simić, M., Manojlović, D., & Jović, V. (2013). SEM/EDX and XRD characterization of silver nanocrystalline thin film prepared from organometallic solution precursor. *Journal of Mining and Metallurgy B: Metallurgy, 49*(1), 91-95.

Edison, T. J. I., & Sethuraman, M. G. (2013). Biogenic robust synthesis of silver nanoparticles using *Punica granatum* peel and its application as a green catalyst for the reduction of an anthropogenic pollutant 4-nitrophenol. *Spectrochimica Acta Part A: Molecular and Biomolecular Spectroscopy, 104*, 262-264.

Kalaiselvi, V., Mathammal, R., Vijayakumar, S., & Vaseeharan, B. (2018). Microwave assisted green synthesis of hydroxyapatite nanorods using *Moringa oleifera* flower extract and its antimicrobial applications. *International Journal of Veterinary Science and Medicine, 6(*2), 286-295.

Kannan, S. K., & Sundrarajan, M. (2014). A green approach for the synthesis of a cerium oxide nanoparticle: characterization and antibacterial activity. *International Journal of Nanoscience, 13*(03), 1450018. doi:10.1142/S0219581X14500185

Karimi, J., & Mohsenzadeh, S. (2015). Rapid, green, and eco-friendly biosynthesis of copper nanoparticles using flower extract of *Aloe vera*. *Synthesis and Reactivity in Inorganic, Metal-Organic, and Nano-Metal Chemistry, 45*(6), 895-898.

Kaviyarasu, K., Mariappan, A., Neyvasagam, K., Ayeshamariam, A., Pandi, P., Palanichamy, R. R., Gopinathan, C., Mola, G. T., & Maaza, M. (2017). Photocatalytic performance and antimicrobial activities of HAp-TiO_2 nanocomposite thin films by sol-gel method. *Surfaces and Interfaces, 6*, 247-255.

Kayani, Z. N., Saleemi, F., & Batool, I. (2015). Effect of calcination temperature on the properties of ZnO nanoparticles. *Applied Physics A, 119*(2), 713-720.

Kumar, P. V., Shameem, U., Kollu, P., Kalyani, R. L., & Pammi, S. V. N. (2015). Green synthesis of copper oxide nanoparticles using *Aloe vera* leaf extract and its antibacterial activity against fish bacterial pathogens. *BioNanoScience, 5*(3), 135-139.

Mahmud, S. A. (2016) Biosynthesis of CeO_2 NPs using the optimal extract of *Moringa olifera*. *International Journal of Chemical and Biochemical Sciences 10*, 37-39.

Mariappan, A., Pandi, P., Balasubramanian, N., Palanichamy, R. R., & Neyvasagam, K. (2017). Structural, optical and antimicrobial activity of copper and zinc doped hydroxyapatite nanopowders using sol-gel method. *Mechanics, Materials Science and Engineering, 9.* doi*:*10.2412*/*mmse.1.46.162

Mittal, S., & Pandey, A. K. (2014). Cerium oxide nanoparticles induced toxicity in human lung cells: Role of ROS mediated DNA damage and apoptosis. *BioMed Research International, 2014*, Article ID 891934. doi:10.1155/2014/891934

Mobeen, A., & Sundaram, R. (2019) Synthesis and characterization of cerium oxide nanoparticles using sucrose as a green capping agent and its application for antibacterial and humidity sensor studies, *International Journal of Research in Advent Technology, 7*(2), 842-848.

Morshed, A. H., Moussa, M. E., Bedair, S. M., Leonard, R., Liu, S. X., & El-Masry, N. (1997). Violet/blue emission from epitaxial cerium oxide films on silicon substrates. *Applied Physic Letters, 70*(13), 1647-1649.

Muralikrishna, T., Pattanayak, M., & Nayak, P. L. (2014). Green synthesis of gold nanoparticles using (*aloe vera*) aqueous extract. *World Journal of Nano Science and Technology*, 3(2), 45-51.

Nisha, S. N., Aysha, O. S., Rahaman, J. S. N., Kumar, P. V., Valli, S., Nirmala, P., & Reena, A. (2014). Lemon peels mediated synthesis of silver nanoparticles and its antidermatophytic activity. *Spectrochimica Acta Part A: Molecular and Biomolecular Spectroscopy, 124*, 194-198.

Niu, J., Azfer, A., Rogers, L. M., Wang, X., & Kolattukudy, P. E. (2007). Cardioprotective effects of cerium oxide nanoparticles in a transgenic murine model of cardiomyopathy. *Cardiovascular research, 73*(3), 549-559. doi:10.1016/j.cardiores.2006.11.031

Sisubalan, N., Ramkumar, V. S., Pugazhendhi, A., Karthikeyan, C., Indira, K., Gopinath, K., & Basha, M. H. G. (2018). ROS-mediated cytotoxic activity of ZnO and CeO_2 nanoparticles synthesized using the Rubia cordifolia L. leaf extract on MG-63

human osteosarcoma cell lines. *Environmental Science and Pollution Research, 25*(11), 10482-10492.

Thovhogi, N., Diallo, A., Gurib-Fakim, A., & Maaza, M. (2015). Nanoparticles green synthesis by *Hibiscus sabdariffa* flower extract: main physical properties. *Journal of Alloys and Compounds, 647*, 392-396.

Vélez, E., Campillo, G., Morales, G., Hincapié, C., Osorio, J., & Arnache, O. (2018). Silver nanoparticles obtained by aqueous or ethanolic aloe Vera extracts: An assessment of the antibacterial activity and mercury removal capability. *Journal of Nanomaterials, 2018* Article ID: 7215210, doi:10.1155/2018/7215210

Wang, L., Ren, J., Liu, X., Lu, G., & Wang, Y. (2011). Evolution of SnO_2 nanoparticles into 3D nanoflowers through crystal growth in aqueous solution and its optical properties. *Materials Chemistry and Physics, 127*(1-2), 114-119.